AN ANTENNA ARRAY FOR THE GALILEO SYSTEM WITH BEAMFORMING CAPABILITIES

E. S. Neves and A. Dreher
German Aerospace Center (DLR) / Institute of Communications and Navigation
Oberpfaffenhofen, 82234 Weßling
Germany

ABSTRACT

This contribution shows the beamforming capabilities of a broadband antenna array designed for the whole Galileo frequency band. In addition, a brief description on the front-end design is presented. The employed beamforming approach, performed by a software developed in DLR, considers a combination of an optimized Chebychev pattern with the Sample Matrix Inversion (SMI) algorithm. It allows the calculation of the excitation currents needed to steer the main beam of an antenna array at the same time it suppresses the side lobe levels to a desired value and generates nulls in the directions where interferers are incoming.

1. INTRODUCTION

The upcoming Galileo satellite system will require improvements on the navigation receiving systems in order to provide more accurate navigation services. Any navigation receiving system begins with the antenna or antenna terminal. In order to obtain the best possible navigation accuracy, exploiting the full capabilities offered by this new system, the design of state-of-the-art antenna systems must be pursuit.

In this paper the most relevant characteristics of the antenna element and array are presented. Also, a brief description of the RF front-end is included, so the reader can have a more complete idea about the smart antenna terminal as a whole. Finally, a number of results describing the beamsteering performance are shown and discussed.

The main requirements for such an antenna terminal are the best possible hemisphere coverage with the best possible polarization purity and good input impedance over the complete frequency range of interest. The specifications in terms of gain, scanning capabilities, input impedance matching, polarization purity and physical size are given by Table 1. The frequency bands of interest are illustrated in Fig. 1 corresponding to the bands E5, E6, E2, L1 and E1 [1]. If the broadband approach is considered, then the total bandwidth becomes 427 MHz centered at 1377.5 MHz, i.e. ≈ 31%. In fact, the broadband approach is the chosen one in this work due to extremely tough requirements regarding the radiation characteristics of the antenna array.

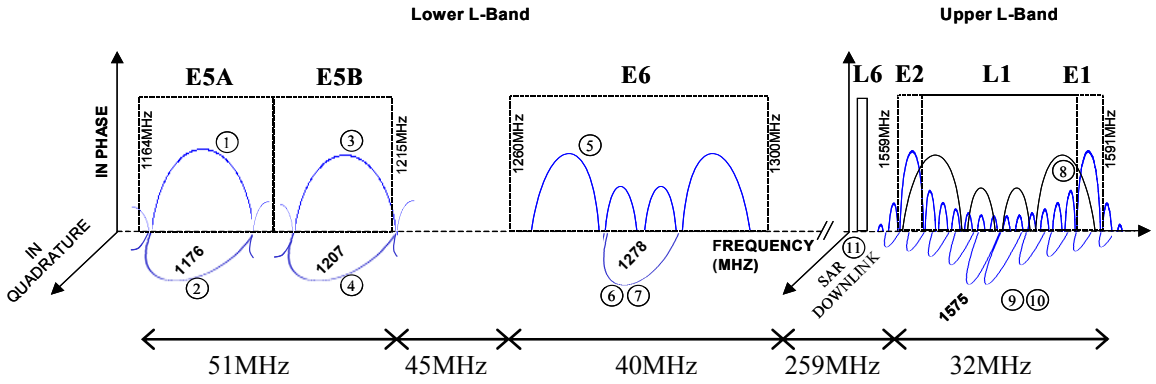

Fig. 1. Galileo frequency spectrum.

Parameter	Specification
Bandwidth	1164 MHz to 1591 MHz (31%)
Return loss	-10 dB min
Polarization	RHCP
Azimuth scanning	360°
Elevation scanning	from 30° to 90° (from 0° to 30° desired)
Gain	10 dBi min. over all scan angles (30° to 90° elevation)
Axial ratio	3 dB min. over all scan angles (30° to 90° elevation)
Cross-polarization	15 dB minimum, 25 dB or better is desirable

Table 1. Antenna array specifications.

2. ANTENNA

Developing an antenna which can operate in all Galileo frequency bands shown by Fig. 1 and that at the same time matches all specifications given in Table 1 can prove to be a very difficult task, especially if other constrains like size, weight and cost are also to be taken into account. Another issue is whether the antenna should be broadband, covering the whole frequency range or multiband covering only the bands of interest separately from each other. Although the second approach seems to be more attractive for the first view due to a potentially better noise and interferers suppression, its known from the literature that multiband antennas usually presents stronger radiation pattern asymmetry and lower polarization purity [2]. These drawbacks could significantly degrade the beamsteering capabilities of an antenna array. Therefore, it was chosen in this work to design a broadband antenna to get the most suitable element for beamforming purposes.

2.1. Antenna element

The specifications for the final antenna array require a high performance antenna element. To achieve the required performance a suitable geometry was proposed [3] and optimized to the project necessities [4]. Such geometry consists of a single circular patch antenna symmetrically fed by four small capacitive coupled circular plates, referred to as feeding plates. They are fed by probes in a sequential phase rotation of 90° steps provided by a combination of one 180° hybrid (rat race) and two 90° hybrids. The complete structure is presented in Fig. 2 where it is possible to observe the circular patch of the antenna, its feeding plates and the feeding hybrids.

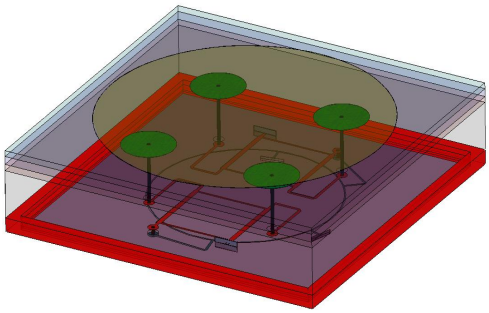

Fig. 2. Single element wire-frame view.

As can be seen in Fig. 2, the feeder system was designed to fit completely under the space delimited by the patch radiator, in order to facilitate the integration for the antenna array design. Fig. 3 shows the antenna element layering including the substrate parameters and the feeding system layers.

Full wave simulations for the antenna including its feeding system were performed showing good results. The return loss stays under 10 dB for the complete specified frequency range, as shown by Fig. 4.

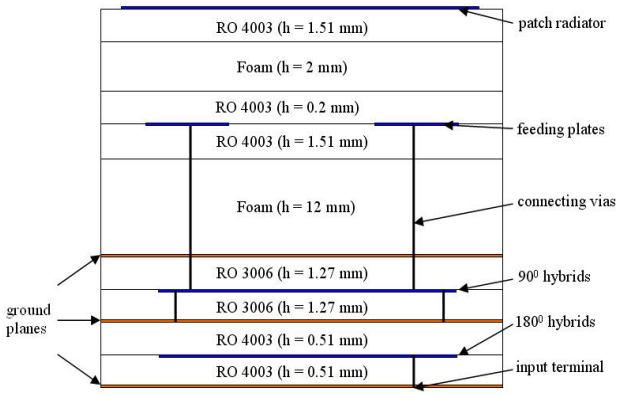

Fig. 3. Single element layering schematic.

Fig. 5 shows the gain patterns at the center frequency of the complete band f_c = 1.377 GHz. It can be seen that the beam is relatively broad and the radiation pattern components are quite symmetric which makes this antenna element very suitable to applications in antenna arrays for beam-steering.

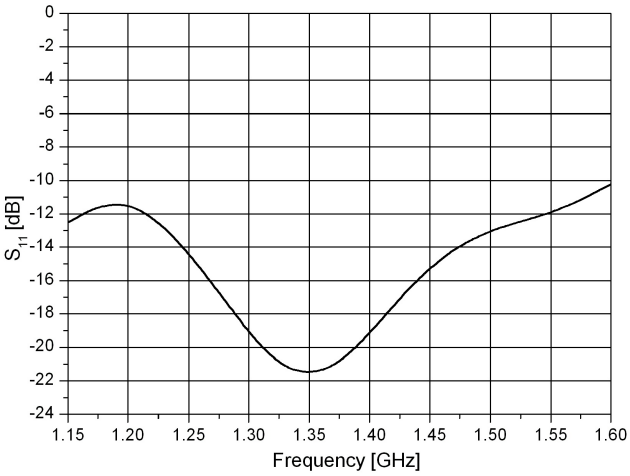

Fig. 4. Element return loss simulation.

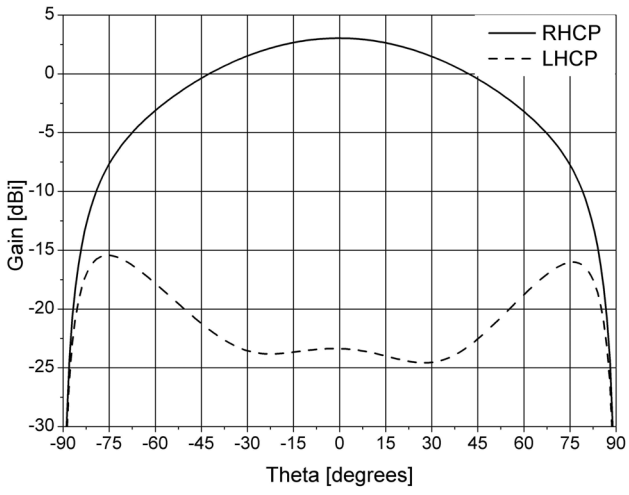

Fig. 5. Element gain patterns at 1.377 GHz simulation.

The gain variation of the antenna element at the broadside direction is about 2 dB over the frequency band of interest. The antenna gain drops very slowly for steering angles up to 60^0, where it reaches 6 dB below maximum. Between 60^0 and 75^0 the gain drops other 4 dB to 5 dB and after 75^0 the gain decreases quickly, which is common for microstrip antennas. The antenna gain versus frequency for several angles is shown by Fig. 6.

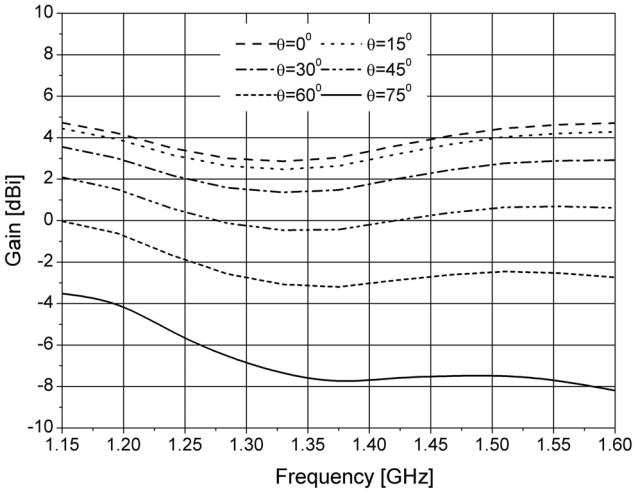

Fig. 6. Element gain over several scan angles simulation.

Following Fig. 7, the axial ratio remains under 4.7 dB for the complete frequency range of interest even for scanning angles up to 75^0. Actually, for angles up to 60^0 the axial ratio remains under 3 dB, being less than 2 dB for angles up to 40 degrees. These excellent results are due to the symmetrical sequential phase rotation in conjunction with an optimized structure.

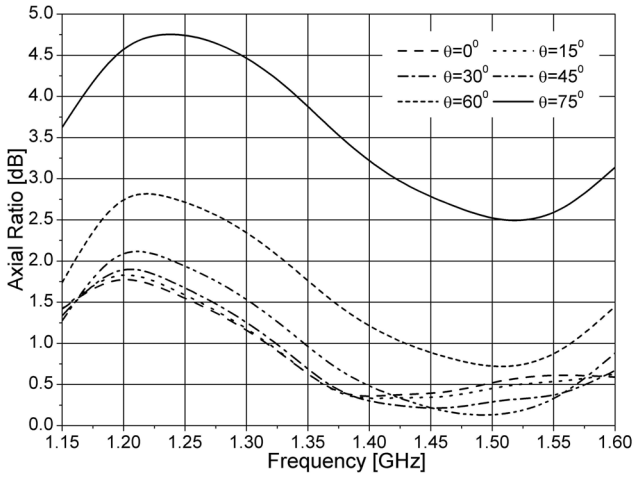

Fig. 7. Element axial ratio over several scan angles simulation.

2.2. Antenna Array

For the antenna array a modular concept is employed. In this concept each antenna element, integrated with its RF front-end modules, is constructed separately and then attached to a metallic frame in order to form the array. Therefore, a great flexibility for tests and measurements is achieved.

A very import constraint for the antenna array is its physical size. Although it is not explicitly listed in the requirements of Table 1, the overall size must be as small as possible in order to make it suitable for mobile applications. Thus a 4 x 4 element antenna array measuring 38 cm x 38 cm was chosen. With such a small number of antenna elements it is not possible to precisely steer the beams towards very low elevation angles. As a matter of fact, the beam pointing keeps relatively good for elevation angles of 30^0 or higher. For lower elevation angles, the incoming signals must be received by a portion of the radiation beam that lies not at its direction of maximum. In this case the reception characteristics will degrade as the elevation angle becomes smaller.

An array schematic is illustrated by Fig. 8. The connection between the upper and the lower modules is done by means of high phase precision coaxial cables.

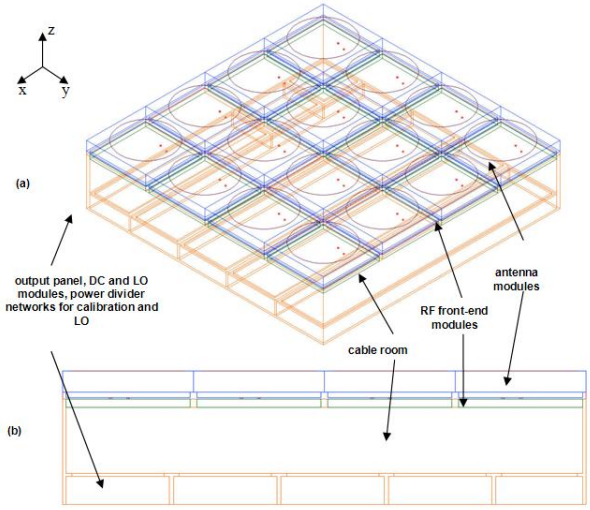

Fig. 8. Antenna array frame structure. (a) Perspective view. (b) Side view.

Fig. 9 shows the gain pattern for three distinct desired beampointing conditions at 1.377 GHz using a uniform distribution for the excitation currents.

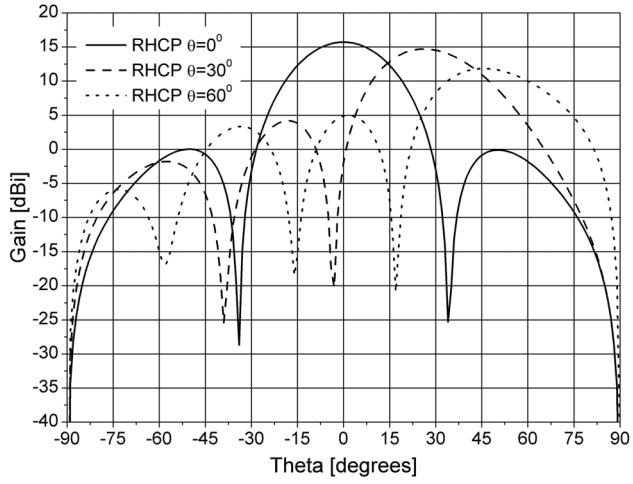

Fig. 9. Beam steering of a 4x4 antenna array at 1.377 GHz simulation.

Due to the limited number of elements it is not possible to point the maximum of the beam to angles greater than 50^0 without generating grating lobes that can be no longer suppressed by any means by the beamforming algorithms. So, for a link between the antenna array and a satellite that lies in an elevation angle smaller than 30^0, the link must be made using a portion of the radiation beam that is not the beam pointing angle, and may even lie out of the HPBW. The axial ratio for the antenna array is very good. According to Fig. 10, it remains under 2 dB for incident angles up to 60^0 and does not exceed 5 dB for incident angles up to 75^0.

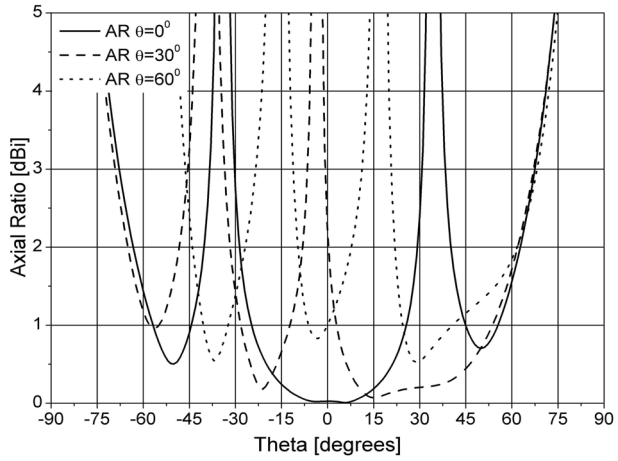

Fig. 10. Axial ratio of a 4x4 antenna array at 1.377 GHz simulation.

These results reinforce the possibility of using portions of the array radiation patterns that lies out of the beam pointing direction.

3. RF FRONT-END

Following the module concept of the smart antenna terminal described above, it is also planned to design a module containing a low-noise RF front-end. Such a module is to be small enough in order to fit underneath each antenna element. In a first stage of the project, a super heterodyne front-end is to be developed while in a second stage, a direct RF sampling architecture will be considered.

Fig. 11 shows in a simplified manner the super heterodyne option. The only difference in the case of a the direct RF sampling is the absence of the down conversion circuitry due to the direct sampling of the RF signal. It was decided to split the signal into the three main bands of interest and process it separately. The front-end gain is between 82 dB and 118 dB and the output power is between -22 dBm and +13 dBm. The intermediate frequency (IF) is set to 61.38 MHz for a sampling rate of 245.52 MHz, exactly four times IF. In addition to allowing the separation of the in-phase (I) and quadrature (Q) components to be made after the analogue to digital conversion, this sampling rate will save a significant amount of FPGA processing because instead of a mathematical operation to get the I and Q components (multiplication by a sine or cosine), they can be directly extracted from the samples.

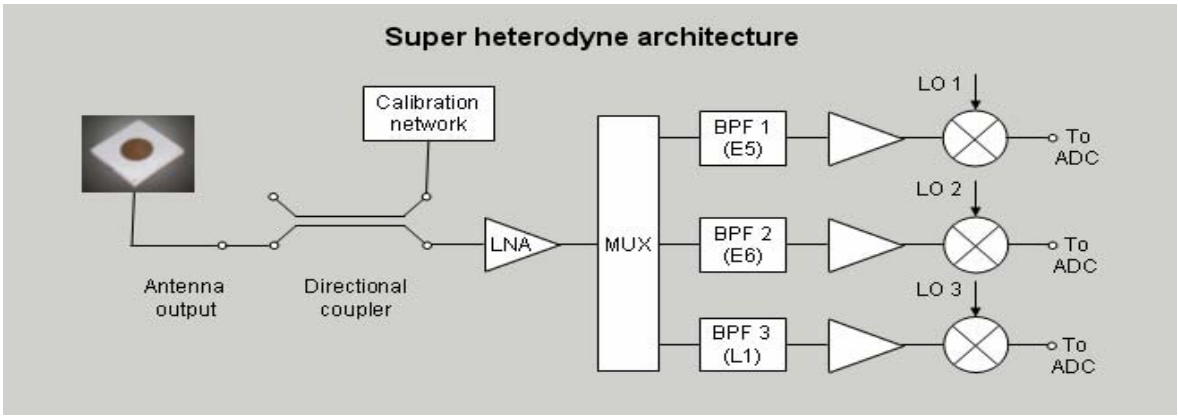

Fig. 11. Super heterodyne RF front-end receiver schematic for the Galileo smart antenna terminal.

4. BEAMFORMING ANALYSES

Simulations for different beamforming conditions and frequencies have been carried out in order to verify the array performance. Among the most important aspects taken into account in these simulations are the influence of the mutual coupling and a beamsteering limit analysis. These two topics will be discussed in the subsequent sections.

In order to include the mutual coupling into the beamforming simulations, the radiation characteristics for each array element were determined using the Planar EM Simulator from Ansoft Designer®. A decoupling algorithm was applied according to the procedure described in [5]. The dielectric layers and ground planes were considered infinite in extension.

Since the array is designed to operate at the entire Galileo band, computations have been performed for frequencies located at the lower and upper parts of it. The first observable effect when working with a broad

band is that the directivity, as well as the side lobe level (SLL) related to the main lobe, may vary significantly from the lower to the upper frequencies. For instance, when pointing the main beam to broadside and without applying any SLL suppression, a directivity of 15.65 dBi is observed at 1.19 GHz in contrast to 17.98 dBi at 1.57 GHz. One reason for that is the inter-element spacing, which is 0.38 λ_0 for the first and 0.5 λ_0 for the second frequency respectively.

Simulations pointing the main beam to a number of elevation angles with SLL suppression of 20 dB were performed. With this setup, the main beam could be steered down to an elevation angle not less then 42°. This is mainly due to the radiation pattern of the single element together with the fact that the number of antenna array elements is limited to only 16.

4.1. Influence of the mutual coupling

Mutual coupling can affect significantly the performance of the smart antenna terminal while performing beamforming. In order to take these effects into account, a software named SEQAR, which was developed by the antenna group, was employed for the beamsteering analyses [5]. Figs. 12 and 13 show us a comparison of a given beamsteering case considering and not considering mutual coupling. As can be observed, the mutual coupling affects the axial ratio the most, while the beam pointing angle is less affected.

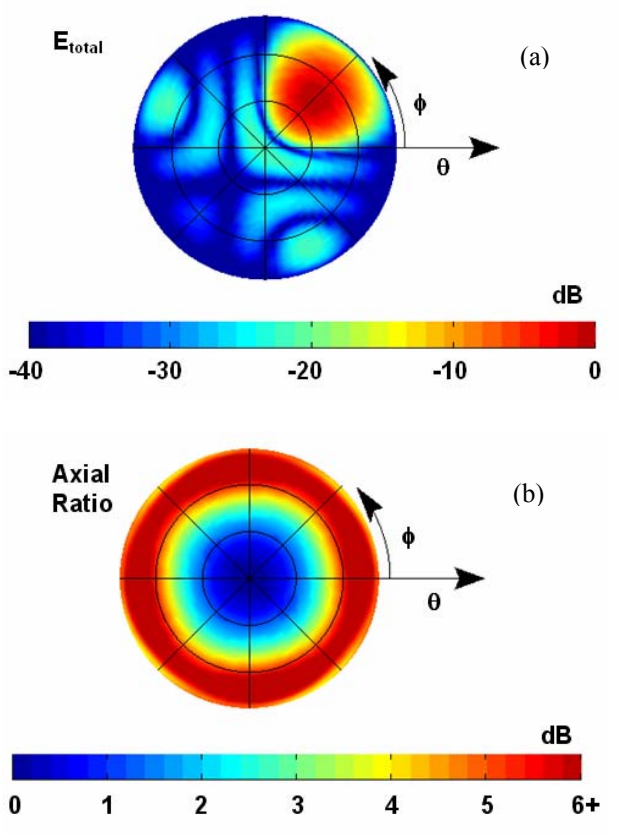

Fig. 12. (a) Radiation pattern and (b) axial ratio pattern pointing at θ = 45° and ϕ = 45° at 1.57 GHz simulation not considering mutual coupling.

However, as shown by Fig. 13b, the axial ratio value for the beampointing angle in question is still around 3 dB, which can be considered a quite positive result. This is be still the case for even lower elevation angles like 20° to 30°.

Another observable effect due to mutual coupling is the degradation of the side lobe levels, which will become higher then in the case without considering mutual coupling.

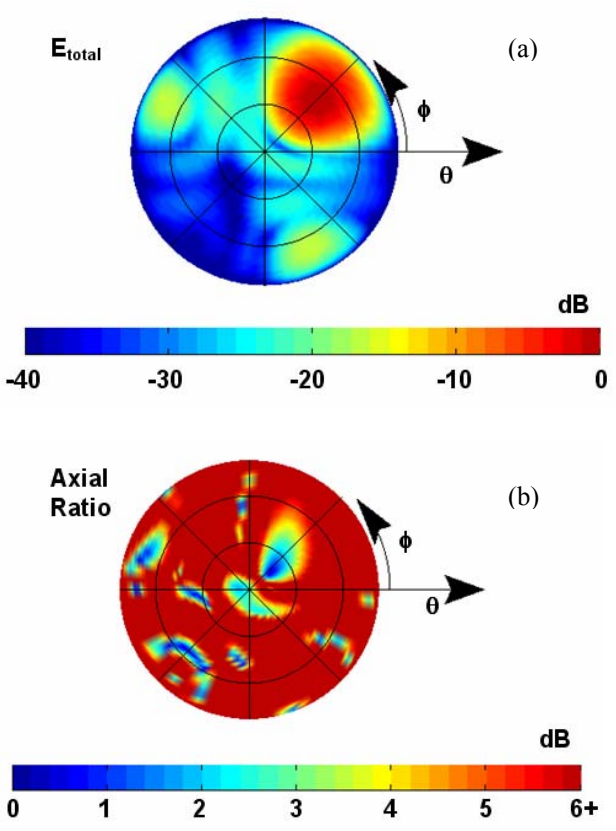

Fig. 13. (a) Radiation pattern and (b) axial ratio pattern pointing at θ = 45° and ϕ = 45° at 1.57 GHz simulation considering mutual coupling.

4.2. Beamsteering limit analysis

The beamsteering capabilities of the Galileo smart antenna terminal are one of the most important aspects to be considered. Therefore, an extensive analysis was performed in order to investigate what are the limitations in terms of maximum steerable angle. Since the antenna array is quite broadband, it is expected that this limitations will significantly depend on the frequency. Indeed the maximum beampointing angle varies from 44° to 48° (from the zenith) with the frequency going from 1.19 GHz to 1.57 GHz. Figs. 14 and 15 show the results in the extremes of this frequency range. The difference in the antenna gain becomes clear when observing the beamwidth from both Figs. 14a and 15a. This is due to the difference in the inter-element spacing in these two distinct frequencies.

Despite the difference on the maximum beampointing angle, it is also possible to observe that for these cases the beamwidth becomes very broad, meaning that the

power level of a received signal coming at lower elevation angles will not be so different than that coming from about 45°. The radiation pattern starts decreasing more rapidly for elevation angles of 15° or less. In the direction of an elevation angle of about 8° the radiation pattern level is approximately 10 dB below the maximum.

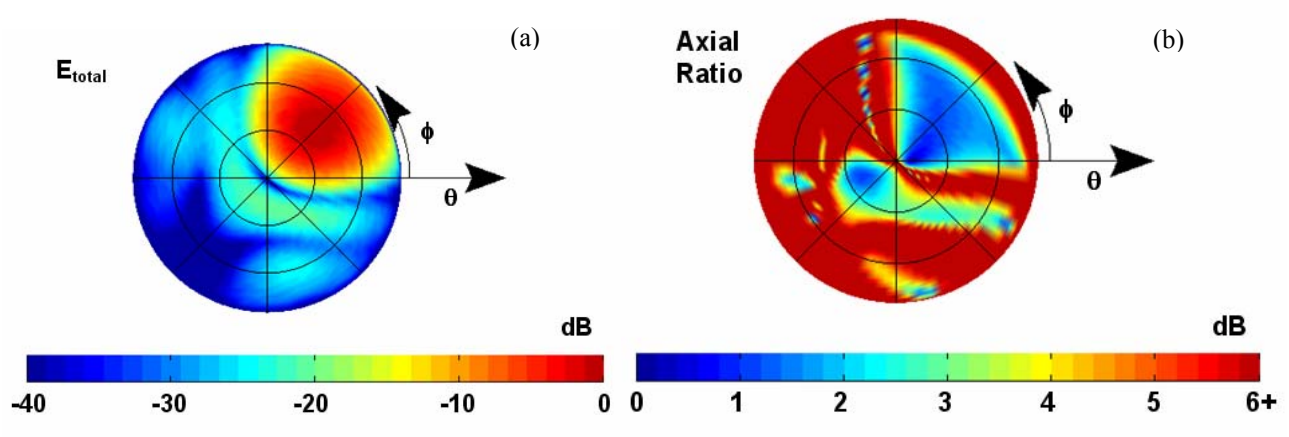

Fig. 14. (a) Radiation pattern and (b) axial ratio pattern for a beampointing at $\theta = 45°$ and $\phi = 45°$ at 1.19 GHz.

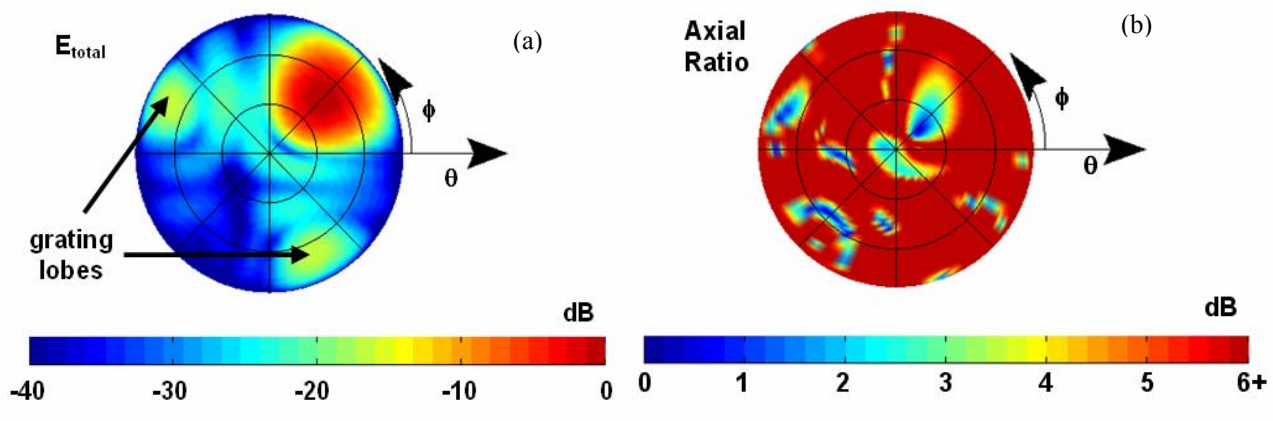

Fig. 15. (a) Radiation pattern and (b) axial ratio pattern for a beampointing at $\theta = 45°$ and $\phi = 45°$ at 1.57 GHz simulation.

4.3. Further results

In order to test the results obtained by the program SEQAR, mentioned in the anterior section, a number of beamsteering cases were selected and beamforming power divider networks were designed according to the output of SEQAR to adjust the excitation phases and amplitudes. Fig. 16 illustrates a given power divider network geometry.

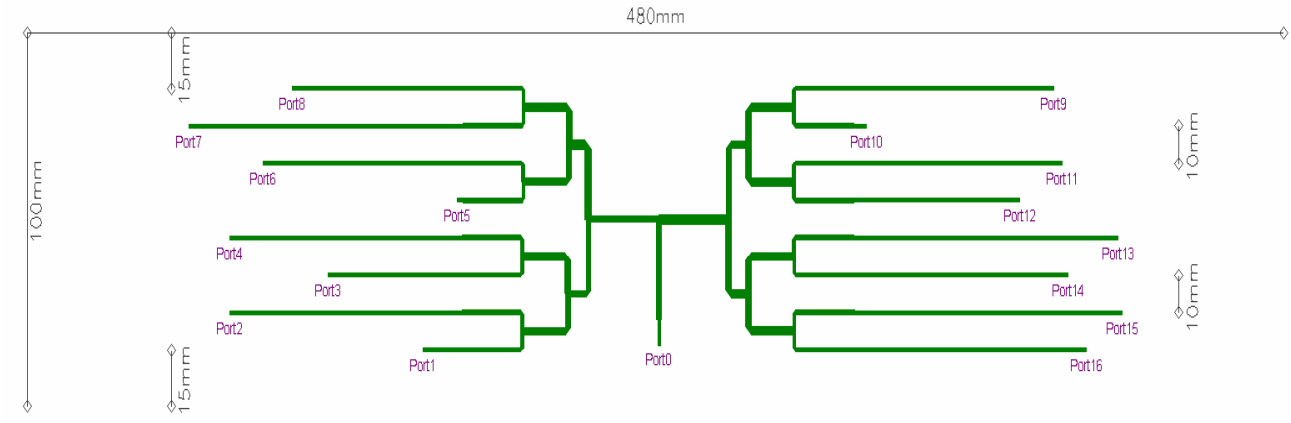

In general, the results obtained from the simulations on Ansoft Designer and HFSS are in very good agreement with the predictions from the SEQAR program. This is illustrated by Figs. 17 and 18, where the results for a beamsteering towards θ = 44° and ϕ = 120° at 1.19 GHz are shown. Here, a quite good precision of the beampointing angle was achieved.

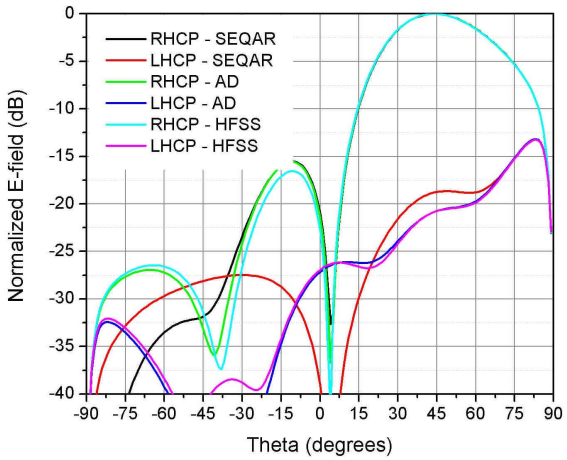

Fig. 17. Radiation patterns for ϕ = 120° cut at 1.19 GHz simulation.

Table 2 shows the excitation coefficients calculated by SEQAR (described as ideal) in order to obtain the beamsteering condition shown by Figs. 17 and 18. The array configuration is shown in Fig. 19 where the elements are indicated according to Table 2. It is possible to observe only small differences in the results obtained from the simulation of the power divider network performed with Ansoft Designer and HFSS to the coefficients provided by SEQAR and therefore the resulting radiation patterns got also very similar.
Fig. 20 shows the full 3D radiation pattern comparison using the coefficients from Table 2. Here it is possible to observe that the good agreement between the results is not only achieved for a particular cut but for the whole radiation pattern.

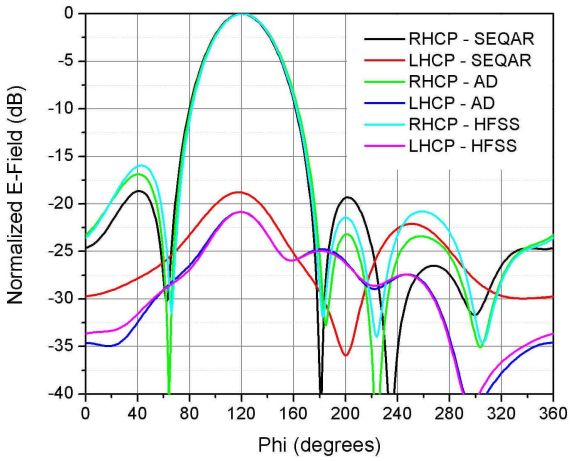

Fig. 18. Radiation patterns for θ = 44° cut at 1.19 GHz simulation.

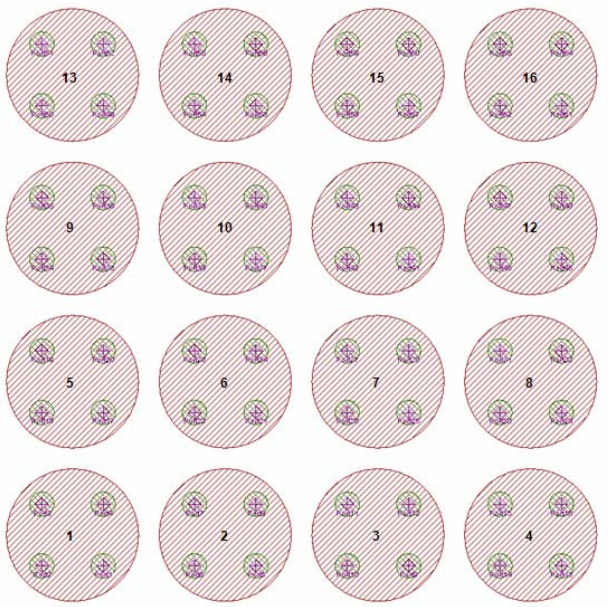

Fig. 19. Antenna array with numbered elements.

Antenna port	13	16	1	4	3	2	15	14	7	9	8	12	5	11	10	6
Divider port	1	2	3	4	5	6	7	8	9	10	11	12	13	14	15	16
Ideal amplitudes (dB)	**-16.83**	**-16.60**	**-16.16**	**-16.16**	**-13.36**	**-12.31**	**-12.31**	**-12.39**	**-11.98**	**-11.82**	**-11.82**	**-11.75**	**-11.53**	**-10.35**	**-9.38**	**-9.84**
Designer amplitudes (dB)	-17.14	-16.99	-16.29	-16.26	-13.58	-12.35	-12.38	-12.17	-11.89	-11.82	-11.73	-11.9	-11.72	-10.55	-9.34	-9.77
HFSS amplitudes (dB)	-16.64	-16.25	-16.07	-15.96	-13.55	-12.52	-12.49	-12.86	-12.19	-11.95	-12.15	-11.85	-11.74	-10.55	-9.89	-10.52
Ideal normalized phase (degrees)	**0**	**173.68**	**-43.28**	**119.16**	**74.92**	**26.86**	**117.75**	**53.83**	**-5.87**	**96.67**	**25.83**	**-75.54**	**-155.79**	**-116.17**	**163.05**	**-76.25**
Simulated normalized phase (degrees)	0	172.7	-44.78	119.06	77.54	27.95	119.24	56.41	-6.34	99.07	25.82	-74.99	-157.71	-115.87	162.59	-73.7

Table 2. Excitation coefficients for the antenna array elements in order to achieve a beamsteering towards θ = 44° and ϕ = 120° at 1.19 GHz.

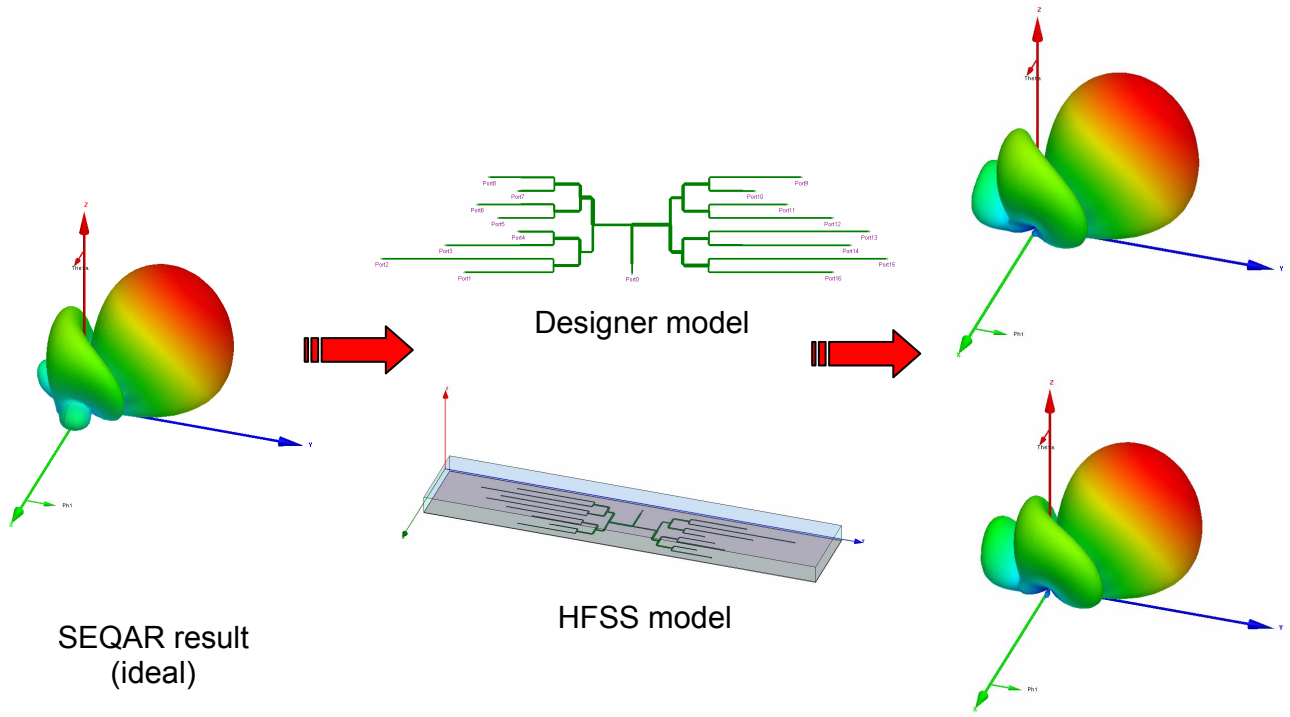

Fig. 20. 3D radiation patterns for a beamsteering towards θ = 44° and ϕ = 120° at 1.19 GHz simulation.

5. CONCLUSION

An extensive study of the beamsteering capabilities of a 4x4 antenna array for the Galileo system has been carried out. Due to the limited number of elements of the array, the scan angle limitation is about 50 degrees. However at that limit the main beam becomes broader and an incoming signal can be received with relatively good gain levels at lower elevation angles. For instance, a gain around 0 dBi could still be achieved for an elevation angle of approximately 8°. Although mutual coupling effects strongly affect the axial ratio, good levels were obtained for the beam pointing angles. The design of passive beamforming tests was successfully done, showing a very good agreement between the simulations results with the different available simulation tools obtained. The next step is to finish the antenna array construction and to measure it with the passive beamforming power dividers, as well as with an active beamformer.

6. REFERENCES

[1] G. W. Hein, J. Godet, J.-L. Issler, J.-C. Martin, P. Erhard, R. L.-Rodriguez and T. Pratt, "Status of Galileo frequency and signal design," *Proc. of ION GPS/GNSS.*, 14 pp. CD-ROM, Portland, Sep. 2002.

[2] E. S. Neves, "Analise e Projeto de Antenas de Microfita Multibanda," *Master Thesis.*, Technological Institute of Aeronautics, Sao Jose dos Campos – Brazil, May 2002.

[3] K. Wong, T. Chiou, "Broad-band single-patch circularly polarized microstrip," *IEEE Trans. Antennas Propagat.*, vol. 49, pp. 41-44, Jan. 2001.

[4] E. S. Neves, P. de Vita and A. Dreher, "Smart antenna arrays for GPS and Galileo applications," *2nd ESA Workshop on Satellite Navigation User Equipment Technologies*, Noordwijk, The Netherlands, Dec. 2004, (8pp. CD-ROM).

[5] M. Clergeaud and M. Thiel, "Algorithms for beamforming and beamsteering of adaptive antennas for satellite communications and navigation," *Internal Report,* DLR-IB 554-04/01, DLR, Germany, 2003.